

Five-dimensional Floquet topological semimetals with emergent Yang monopoles and linked Weyl surfaces

Zheng-Rong Liu,¹ Rui Chen,^{1,*} and Bin Zhou^{1,2,†}

¹*Department of Physics, Hubei University, Wuhan 430062, China*

²*Key Laboratory of Intelligent Sensing System and Security of Ministry of Education, Hubei University, Wuhan 430062, China*

(Dated: January 8, 2025)

Recently, Floquet topological matter has attracted significant attention for its potential to reveal novel topological phases inaccessible in static systems. In this paper, we investigate the effect of a time-periodic driving on the five-dimensional (5D) normal insulators. We show that the time-periodic driving can induce a topological phase transition from a **TP** (time reversal combined with space inversion) symmetry-preserving normal insulator to a 5D Floquet topological semimetal with emergent Yang monopoles characterized by the second Chern number. Additionally, we show that this time-periodic driving can also lead to a topological phase transition from a **TP** symmetry-breaking normal insulator to a 5D Floquet topological semimetal with a Hopf link formed by Weyl surfaces. Besides, further increasing the strength of the time-periodic driving, the two 5D Floquet topological semimetal phases are transformed into the 5D Floquet Chern insulators. Our paper is helpful for future studies in higher dimensional Floquet systems.

I. INTRODUCTION

Topological semimetals are a class of gapless topological matter that have drawn significant research interest both theoretically and experimentally [1–4]. Topological semimetals not only exhibit a rich variety of bulk and surface transport phenomena but also act as intermediate states during topological phase transitions between distinct gapped topological materials [5–12]. In three dimensions, topological semimetals are classified as Dirac semimetals [13–25], Weyl semimetals [26–42], and nodal-line semimetals [18, 43–47]. In Weyl semimetals, non-degenerate valence and conduction bands touch each other at zero-dimensional (0D) Weyl points. Weyl points appear in pairs and exhibit opposite chiralities [5, 9, 35], with the chirality determined by the first Chern number $C_1 = \frac{1}{2\pi} \oint_{S^2} F d^2\mathbf{k}$ [9, 31, 48–51], where S^2 is the closed two-dimensional (2D) sphere enclosing the Weyl point and F is the Berry curvature. Moreover, there are surface Fermi arcs connecting the projections of the opposite chiral Weyl points [9, 31, 52].

Later, Lian and Zhang generalized three-dimensional (3D) Weyl semimetals to five dimensions [53]. According to the symmetries, a five-dimensional (5D) topological semimetal can be classified into two distinct categories: those hosting 0D Yang monopoles [54–58] and those hosting 2D linked Weyl surfaces [53, 58–65]. When the **TP** (time reversal combined with space inversion) symmetry is preserved, the conduction and valence bands intersect at Yang monopoles. The Yang monopole carries a nonzero second Chern number $C_2 = \frac{1}{8\pi^2} \oint_{S^4} (\Omega \wedge \Omega) d^4\mathbf{k}$ [55, 57, 65, 66], where S^4 is the closed four-dimensional (4D) manifold enclosing the Yang monopole and Ω is the non-Abelian Berry curvature. When the **TP** symmetry is broken, the 0D Yang monopoles evolve into 2D linked Weyl surfaces, and these Weyl surfaces form a Hopf link with

a topological linking number equal to the second Chern number [53, 59, 63].

Floquet topological phases, which are referred to the periodic driving induced topological states, have been widely investigated in lower dimensions [67–100]. Specifically, Floquet topological semimetals possess novel topological properties without analogs in static systems [79, 101–125]. For example, in static systems, a Weyl semimetal must host at least one pair of Weyl points with opposite chirality [48, 49], while the Floquet topological semimetal supports the existence of a single Weyl point [105, 106]. Experimentally, Floquet topological semimetals have been realized in various metamaterials [67, 69, 70, 126–136]. However, research on Floquet topological semimetals has been largely confined to 2D or 3D systems, and higher-dimensional Floquet topological semimetals remain unexplored.

In this paper, we investigate the effects of a time-periodic driving on the 5D **TP** symmetry-preserving (symmetry-breaking) normal insulator. We focus on topological phase transitions in the resonant quasienergy region, where the Floquet sidebands overlap with the original bands as shown in Figs. 1(a) and 1(f). First, we introduce the time-periodic driving to the 5D **TP** symmetry-preserving normal insulator. In the 5D momentum space, the bulk gapless points form a closed 4D manifold because of the bands overlapping in the resonant quasienergy region, which is projected as a closed 2D sphere in the (k_1, k_3, k_5) subspace as shown in Fig. 1(b). Meanwhile, the time-periodic driving induces the coupling between the Floquet sidebands and the original bands, resulting in the 4D manifold collapsing into two 0D gapless points located on the k_5 axis as shown in Figs. 1(c)–(e). These two 0D gapless points are confirmed to be Yang monopoles characterized by the second Chern number. Besides, we find there exist surface Weyl arcs connecting these two 0D Yang monopoles. These features suggest that the time-periodic driving induces a 5D Floquet topological semimetal with Yang monopoles.

Second, we introduce the time-periodic driving to the 5D **TP** symmetry-breaking normal insulator. In the 5D momentum space, the 4D manifold splits into three 4D manifolds

* chenr@hubu.edu.cn

† binzhou@hubu.edu.cn

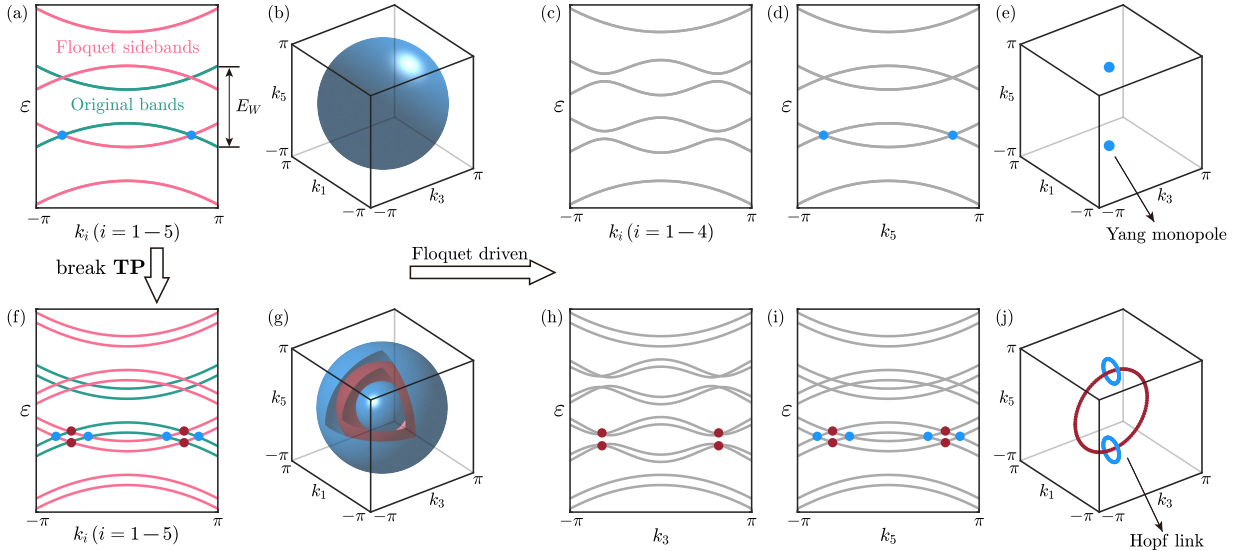


FIG. 1. (a) The quasienergy ε of the Floquet system as a function of k_i ($i = 1, 2, 3, 4, 5$) when the strength of time-periodic driving $m_t = 0$. In the presence of the **TP** symmetry, the bulk bands are twofold degenerate. The green and pink lines indicate the original bands of $H(\mathbf{k})$ and the Floquet sidebands of $H(\mathbf{k}) \pm \omega$, respectively, where ω is the frequency of time-periodic driving. When $\omega < E_W$, they intersect at the light blue points in the resonant quasienergy region, and E_W represents the bandwidth of the static Hamiltonian $H(\mathbf{k})$. (b) The light blue gapless points form a closed spherical surface in the (k_1, k_3, k_5) subspace when (k_2, k_4) are fixed. (c)-(e) When $m_t \neq 0$, the Floquet sidebands couple with the original bands, resulting in the bulk gap being opened in the first Brillouin zone, except for two 0D Yang monopoles located on the k_5 axis. Similar evolutionary processes are shown in (f)-(j) when the **TP** symmetry is broken. (f) In the absence of the **TP** symmetry, the degeneracy of the bulk bands is destroyed. In the resonant quasienergy region, there are bulk gapless points marked by the light blue dots between bands 4 and 5, and by the red dots between bands 5 and 6 (or bands 3 and 4). (g) The bulk gapless points form three concentric spherical surfaces. (h)-(j) When $m_t \neq 0$, the time-periodic driving forces the bulk gap to open, except for a Hopf link formed by linked Weyl surfaces.

since the band degeneracy is broken. As shown in Fig. 1(g), the projections of these three 4D manifolds in the (k_1, k_3, k_5) subspace appear as three concentric spheres. Meanwhile, the time-periodic driving forces the three 4D manifolds to shrink into the 2D linked Weyl surfaces. In Fig. 1(j), the red and light blue loops are the projections of the Weyl surfaces shown in the (k_1, k_3, k_5) subspace. These linked Weyl surfaces form a Hopf link with the topological linking number equal to the second Chern number, which is equal to the number of surface Weyl arcs. Additionally, both the two 5D Floquet topological semimetals transition into 5D Floquet Chern insulators by further increasing the strength of the time-periodic driving.

The paper is organized as follows. In Sec. II, a 5D time-dependent model and the method for calculating the second Chern number are presented. In Sec. III, numerical calculations show that the effect of the time-periodic driving on the **TP** symmetry-preserving normal insulator, and a 5D Floquet topological semimetal with Yang monopoles is proposed. In Sec. IV, a 5D Floquet topological semimetal with linked Weyl surfaces induced by the time-periodic driving is proposed. In Sec. V, we summarize our results.

II. MODEL AND METHOD

The time-dependent 5D topological semimetal model is given by

$$H(\mathbf{k}, t) = H(\mathbf{k}) + M(t). \quad (1)$$

The first term in Eq. (1) represents a static Hamiltonian describing the 5D topological semimetal [59],

$$H(\mathbf{k}) = \sum_{j=1}^5 \xi_j(\mathbf{k}) \gamma_j + b \frac{i[\gamma_3, \gamma_4]}{2}, \quad (2)$$

where $\xi_j(\mathbf{k}) = \sin(k_j)$ for $j = 1, 2, 3, 4$ and $\xi_5(\mathbf{k}) = m + \sum_{j=1}^4 [1 - \cos(k_j)] + \eta[1 - \cos(k_5)]$. The gamma matrices are written as $\gamma_1 = \sigma_3 \otimes \sigma_1$, $\gamma_2 = \sigma_3 \otimes \sigma_2$, $\gamma_3 = \sigma_3 \otimes \sigma_3$, $\gamma_4 = \sigma_1 \otimes \sigma_0$, and $\gamma_5 = \sigma_2 \otimes \sigma_0$. σ_0 and σ_j ($j = 1, 2, 3$) are identity matrix and Pauli matrices, respectively. m and η are the tuning parameters. In the subsequent calculations, $\eta = 0.5$. The second term in Eq. (1) represents the time-periodic on-site potential $M(t) = m_t \cos(\omega t) \gamma_5$, where m_t and ω are the strength and frequency of the time-periodic on-site potential, respectively.

The first term in Eq. (2) describes a 5D topological semimetal with the **TP** symmetry $\mathcal{TP} = \sigma_1 \otimes \sigma_2 \mathcal{K}$, where time-reversal symmetry $\mathcal{T} = i\gamma_2 \mathcal{K}$ and space-inversion symmetry $\mathcal{P} = \gamma_5$ satisfy $\mathcal{T}H(\mathbf{k})\mathcal{T}^{-1} = H(-\mathbf{k})$ and $\mathcal{P}H(\mathbf{k})\mathcal{P}^{-1} = H(-\mathbf{k})$, respectively. When the second term $b \neq 0$ in Eq. (2), the **TP** symmetry is broken. When $m > b$, the static system is a 5D normal insulator [59].

In 3D Weyl semimetals, there are pairs of Weyl points that carry topological monopole charges given by the first Chern number in the momentum space [48], and the 2D planes in the 3D Brillouin zone that lie between the pair of Weyl points have nonzero first Chern numbers [137]. Moreover, there are sur-

face Fermi arcs connecting the projections of the oppositely charged Weyl points [9]. Similar to the 3D Weyl semimetal, the 5D topological semimetal hosts topologically protected Weyl arcs on its 4D boundaries, and the arcs connect the projections of the two Yang monopoles or Weyl surfaces [53, 59]. The Yang monopole or the Weyl surface is characterized by a nonzero second Chern number C_2 , and the second Chern number in a 4D momentum space (k_1, k_2, k_3, k_4) is given by [55, 138–145]

$$C_2 = \frac{1}{4\pi^2} \int_V d^4\mathbf{k} \text{Tr}[\Omega_{12}\Omega_{34} + \Omega_{41}\Omega_{32} + \Omega_{31}\Omega_{24}], \quad (3)$$

where V represents the first Brillouin zone of the 4D momentum space. The non-Abelian Berry curvature is

$$\Omega_{pq}^{\alpha\beta} = \partial_p A_q^{\alpha\beta} - \partial_q A_p^{\alpha\beta} + i[A_p, A_q]^{\alpha\beta}, \quad (4)$$

where $p, q = 1, 2, 3, 4$, and the Berry connection of the occupied bands is

$$A_p^{\alpha\beta} = -i \langle u^\alpha(\mathbf{k}) | \frac{\partial}{\partial k_p} | u^\beta(\mathbf{k}) \rangle. \quad (5)$$

$|u^\alpha(\mathbf{k})\rangle$ denotes the occupied eigenstates below the Fermi energy ε_F with $\alpha = 1, \dots, N_{\text{occ}}$.

III. 5D FLOQUET TOPOLOGICAL SEMIMETAL WITH YANG MONOPOLES

In this section, we explore the topological phase transition of the 5D Floquet system by applying a time-periodic driving to the **TP** symmetry-preserving normal insulator. Using Floquet theory [146], the time-dependent Hamiltonian $H(\mathbf{k}, t)$ in Eq. (1) can be expressed as the Floquet Hamiltonian H_F through Fourier transformation. The Floquet Hamiltonian H_F is given by

$$H_F = \begin{pmatrix} \ddots & \vdots & \vdots & \vdots & \ddots \\ \cdots & H_{-1,-1} - \omega & H_{-1,0} & H_{-1,1} & \cdots \\ \cdots & H_{0,-1} & H_{0,0} & H_{0,1} & \cdots \\ \cdots & H_{1,-1} & H_{1,0} & H_{1,1} + \omega & \cdots \\ \ddots & \vdots & \vdots & \vdots & \ddots \end{pmatrix}, \quad (6)$$

where

$$H_{n,n'} = \frac{1}{T} \int_0^T H(\mathbf{k}, t) e^{i(n'-n)\omega t} dt \quad (7)$$

with $n, n' = 0, \pm 1, \pm 2, \dots$ is the harmonic component of the time-dependent Hamiltonian $H(\mathbf{k}, t)$, and $T = \frac{2\pi}{\omega}$. In this paper, $H_{n,n} = H(\mathbf{k})$, $H_{n,n\pm 1} = \frac{m_t}{2}\gamma_5$, and $H_{n,n\pm l} = 0$ ($l \geq 2$). Then, we can obtain a $(2n_t+1)N_{\text{band}} \times (2n_t+1)N_{\text{band}}$ effective Floquet Hamiltonian by truncating the Floquet space. $N_{\text{band}} = 4$ is the number of energy bands of the static system. n_t is a positive integer, representing the truncation number [147], and $n, n' \in [-n_t, n_t]$. In subsequent calculations, we select the truncation number $n_t = 1$.

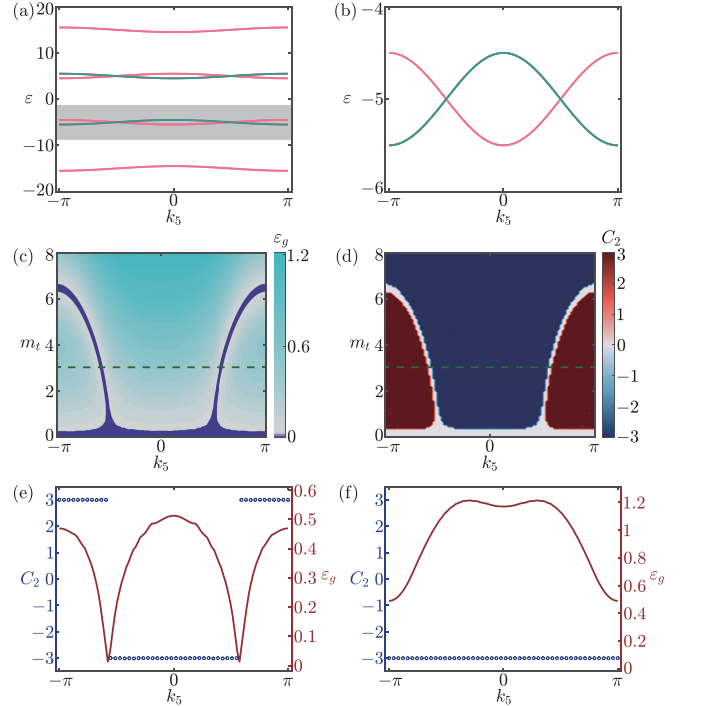


FIG. 2. Topological phases in the Floquet system with the **TP** symmetry. (a) The bulk quasienergy ε as a function of k_5 when $m_t = 0$ and $(k_1, k_2, k_3, k_4) = (\pi, \pi, 0, 0)$. The green (pink) line represents the band of the diagonal block H_0 ($H_0 \pm \omega$) in the Floquet Hamiltonian H_F . The gray region is the resonant quasienergy region we are concerned with. (b) The quasienergy spectra of the gray region in (a). (c) The bulk gap ε_g in the plane (m_t, k_5) when $N_{\text{occ}} = 4$. (d) The second Chern number C_2 in the plane (m_t, k_5) when $N_{\text{occ}} = 4$. (e)–(f) The k_5 -dependent second Chern number C_2 (blue circles) and the bulk gap ε_g (red line). The amplitude of the time-periodic driving for (e) and (f) is $m_t = 3$ and $m_t = 8$, respectively. Here, we choose $\eta = 0.5$, $m = 0.5$, $b = 0$, and $\omega = 10$.

The frequency of the time-periodic driving is in the interval $[E_W/2, E_W]$, where $E_W = 2(m+b) + 18$ represents the band width of the static system. When $E_W/2 < \omega < E_W$, the original bands of $H_{0,0}$ and the Floquet sidebands of $H_{n,n} \pm \omega$ ($n = \pm 1$) overlap each other as shown in Fig. 2(a). By modulating the strength of the time-periodic driving m_t , we study the topological phase transition in the resonant quasienergy region [the gray region in Fig. 2(a)].

In Fig. 2(c), we show the bulk gap ε_g as a function of m_t and k_5 , with the green dashed line given by $m_t = 3$. The dark blue region in the color bar represents the bulk gap tending to zero. When the strength of the time-periodic driving is weak, the bulk band is gapless for any k_5 . When m_t is increased to a suitable strength, there are only two gapless points in the first Brillouin zone. Using k_5 as a parameter, we show the evolution of the second Chern number C_2 on the (k_5, m_t) plane as shown in Fig. 2(d). Compared with Fig. 2(c), it can be found that the second Chern number exhibits a nonzero integer in the gapped regions. In Fig. 2(e), we show the changes in the bulk gap ε_g and the second Chern number C_2 with respect to k_5 when $m_t = 3$. It can be observed that there are only

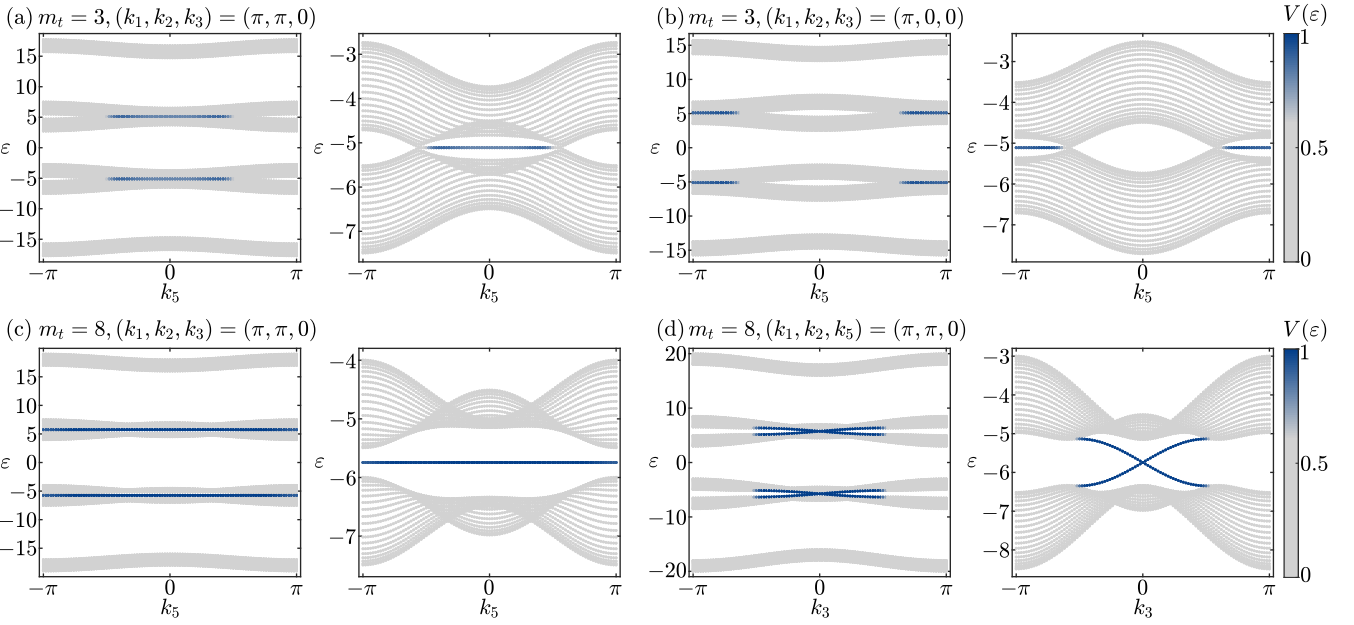


FIG. 3. Quasienergy spectra of the Floquet system when the open boundary condition is along the k_4 direction. (a) The quasienergy spectra as a function of k_5 in the left panel when $m_t = 3$ and $(k_1, k_2, k_3) = (\pi, \pi, 0)$. (b) The quasienergy spectra as a function of k_5 in the left panel when $m_t = 3$ and $(k_1, k_2, k_3) = (\pi, 0, 0)$. (c) The quasienergy spectra as a function of k_5 in the left panel when $m_t = 8$ and $(k_1, k_2, k_3) = (\pi, \pi, 0)$. (d) The quasienergy spectra as a function of k_3 in the left panel when $m_t = 8$ and $(k_1, k_2, k_5) = (\pi, \pi, 0)$. In all plots, the right panel shows the spectra within the resonant quasienergy region of the left panel. The color bar corresponds to the quantity $V(\varepsilon) = \sum_{j \in N_{\text{edge}}} |\phi_j(\varepsilon)|^2 / \sum_{j \in N_{\text{total}}} |\phi_j(\varepsilon)|^2$ for the localization degree at the boundary, where $\phi_j(\varepsilon)$ is the element of the eigenstate with the quasienergy ε at site j . Here, we choose $\eta = 0.5$, $m = 0.5$, $b = 0$, and $\omega = 10$.

two gapless points located on the k_5 axis. With the gapless points as boundaries, the second Chern number near $k_5 = 0$ manifests as a quantized integer $C_2 = -3$, while the second Chern number near $k_5 = \pm\pi$ is $C_2 = 3$. In Fig. 3, we show that the quasienergy spectra of the Floquet system when the open boundary condition is along the k_4 direction. When $m_t = 3$, there are surface Weyl arcs connecting the projections of the bulk gapless points as shown in Figs. 3(a) and 3(b). These features suggest that the time-periodic driving induces a 5D Floquet topological semimetal, with the bulk gapless points being Yang monopoles. In the region near $k_5 = 0$, the surface Weyl arcs are distributed at $(k_1, k_2, k_3) = (\pi, \pi, 0)$, $(k_1, k_2, k_3) = (\pi, 0, \pi)$, and $(k_1, k_2, k_3) = (0, \pi, \pi)$, while in the region near $k_5 = \pm\pi$, the surface Weyl arcs are distributed at $(k_1, k_2, k_3) = (\pi, 0, 0)$, $(k_1, k_2, k_3) = (0, \pi, 0)$, and $(k_1, k_2, k_3) = (0, 0, \pi)$. The number and positions of the surface Weyl arcs are related to the value and sign of the second Chern number.

By further increasing the strength of the time-periodic driving, the bulk gap is opened. In Fig. 2(f), we show the bulk gap ε_g and the second Chern number C_2 as functions of k_5 when $m_t = 8$. For any k_5 , the second Chern number is always $C_2 = -3$. Clearly, this bulk gap opened by the time-periodic driving is topologically nontrivial. Figures 3(c) and 3(d) respectively show the quasienergy spectra as a function of k_5 and k_3 with open boundary conditions along the k_4 direction. In Fig. 3(c), it can be observed that when $(k_1, k_2, k_3) = (\pi, \pi, 0)$, there is a flat band along the k_5 axis within the bulk gap.

Notably, there are also flat boundary states along the k_5 axis when $(k_1, k_2, k_3) = (\pi, 0, \pi)$ or $(k_1, k_2, k_3) = (0, \pi, \pi)$. In Fig. 3(d), there are gapless boundary states in the bulk gap when $(k_1, k_2, k_5) = (\pi, \pi, 0)$. Combining the second Chern number and the quasienergy spectra, we demonstrate that this system is a 5D Floquet Chern insulator characterized by $C_2 = -3$.

IV. 5D FLOQUET TOPOLOGICAL SEMIMETAL WITH LINKED WEYL SURFACES

In this section, we investigate the effects of the time-periodic driving on the 5D TP symmetry-breaking normal insulator. In Fig. 4, we present the evolution of the bulk gap ε_g and the second Chern number C_2 in the plane (m_t, k_5) and the plane (b, k_5) , aiming to study the effect of the strength of the time-periodic driving on the TP symmetry-breaking system, as well as the effect of the TP symmetry-breaking term on the 5D Floquet topological semimetal.

When $E_W/2 < \omega < E_W$, the original bands of $H_{0,0}$ and the Floquet sidebands of $H_{n,n} \pm \omega$ ($n = \pm 1$) overlap each other, resulting in the bulk gap $\varepsilon_g = 0$ when $m_t = 0$ and $N_{\text{occ}} = 4$ as shown in Fig. 4(a). When $m_t = 3$ and $(k_2, k_4) = (\pi, \pi)$, there are two Weyl surfaces (light blue loops) distributed along the k_5 axis, as shown in Fig. 5(a). Meanwhile, there is another Weyl surface (red loops) in the (k_1, k_3, k_5) subspace for $N_{\text{occ}} = 5$, which links with the light blue Weyl surfaces. Obviously, when $(k_2, k_4) = (\pi, \pi)$, a sin-

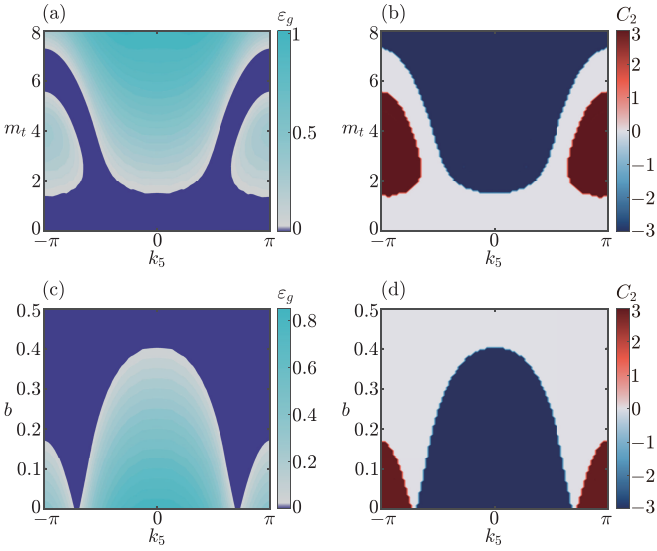


FIG. 4. Phase diagram in the **TP** symmetry-breaking Floquet system. (a) The bulk gap ε_g in the plane (m_t, k_5) . (b) The second Chern number C_2 in the plane (m_t, k_5) . In (a) and (b), $b = 0.1$. (c) The bulk gap ε_g in the plane (b, k_5) . (d) The second Chern number C_2 in the plane (b, k_5) . In (c) and (d), $m_t = 5$. Here, we choose the number of the occupied states $N_{\text{occ}} = 4$, $\eta = 0.5$ and $\omega = 10$.

gle Hopf link appears in the (k_1, k_3, k_5) subspace near $k_5 = 0$, as shown in Fig. 5(a). By varying k_2 and k_4 , we identify six Hopf links in the full 5D momentum space, with three located near $k_5 = 0$, and the remaining three near $k_5 = \pm\pi$. Consequently, the linking numbers of the Weyl surfaces for $N_{\text{occ}} = 4$ in both the $k_5 = 0$ and $k_5 = \pm\pi$ regions are equal to three. A comparison with Fig. 4(b) reveals that the linking number of the Weyl surfaces corresponds to the value of the second Chern number, with opposite signs reflecting distinct Hopf link distributions. We thus characterize this system as a 5D Floquet topological semimetal with linked Weyl surfaces. Moreover, with increasing m_t , the two gapless regions move along the $+k_5$ direction and $-k_5$ directions, respectively, until they eventually coalesce into a single gapless region near $k_5 = \pm\pi$ as shown in Fig. 4(a). This indicates that the two light blue Weyl surfaces merge into a single Weyl surface, as shown in Fig. 5(b). When $m_t = 8$, the bulk gap is opened for $N_{\text{occ}} = 4$, while for $N_{\text{occ}} = 5$, the closed Weyl surface transforms into a cylindrical Weyl surface, as shown in Fig. 5(c). Then, the system becomes a 5D Floquet Chern insulator with $C_2 = -3$.

On the other hand, we find that the **TP** symmetry-breaking term can induce phase transitions in the Floquet system. Figures 4(c) and 4(d) show the bulk gap and the second Chern number as functions of k_5 and b . When $b = 0$, it can be found that there are two bulk gapless points in the 5D first Brillouin zone as shown in Fig. 5(d). Along the k_5 axis, the second Chern number between these two gapless points exhibits two different nonzero integers in the regions near $k_5 = 0$ and $k_5 = \pm\pi$, indicating that the system is a Floquet topological semimetal with two Yang monopoles as shown in Sec. III. When $b > 0$, the 0D Yang monopoles extend into 2D closed

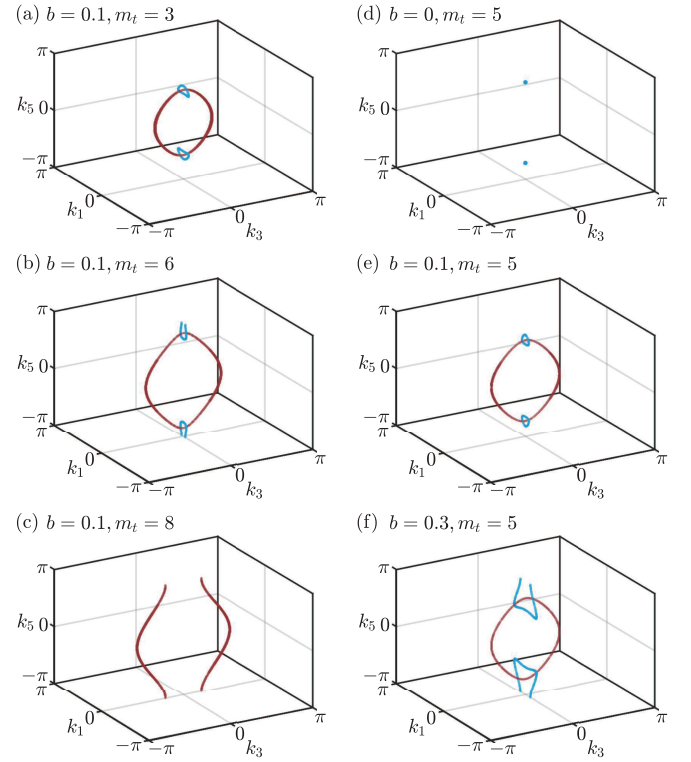


FIG. 5. The distribution of bulk gapless points in the (k_1, k_3, k_5) subspace for (a) $b = 0.1, m_t = 3$; (b) $b = 0.1, m_t = 6$; (c) $b = 0.1, m_t = 8$; (d) $b = 0, m_t = 5$; (e) $b = 0.1, m_t = 5$; and (f) $b = 0.3, m_t = 5$. In (a)–(f), $k_2 = k_4 = \pi$. The red (light blue) loops represent the Weyl surfaces between bands 5 and 6 (between bands 4 and 5). Here, we choose $\eta = 0.5$ and $\omega = 10$.

Weyl surfaces (light blue loops), as shown in Fig. 5(e), thereby transforming the Floquet topological semimetal with Yang monopoles into a Floquet topological semimetal with linked Weyl surfaces. As b increases further, the two Weyl surfaces move closer together along the k_5 axis until they merge into one as shown in Fig. 5(f). When b exceeds a critical value, the bulk gap completely closes for all k_5 , and the system transitions into a trivial metal phase.

V. CONCLUSIONS

In this paper, we investigate the effects of a on-site time-periodic driving on the 5D **TP** symmetry-preserving (symmetry-breaking) normal insulator. First, we investigate the effects of the on-site time-periodic driving on the 5D **TP** symmetry-preserving normal insulator. Our calculations show that the time-periodic driving can induce a topological phase transition from the normal insulator to a 5D Floquet topological semimetal with Yang monopoles. We find that the second Chern number between the two Yang monopoles is a nonzero integer, with its magnitude and sign reflecting the number and position of the surface Weyl arcs, respectively. As the strength of the time-periodic driving increases, the two Yang monopoles gradually approach and eventually annihilate.

Then the bulk gap reopens, and the system transitions from the 5D Floquet topological semimetal to a 5D Floquet Chern insulator characterized by $C_2 = -3$.

Second, we investigate the effects of the time-periodic driving on the 5D **TP** symmetry-breaking normal insulator. We find that the time-periodic driving can induce a transition from the normal insulator to a Floquet topological semimetal with linked Weyl surfaces, and even to a Floquet Chern insulator characterized by $C_2 = -3$. Moreover, we observe that the **TP** symmetry-breaking term can modulate the topological phases of the 5D Floquet topological semimetal. When the **TP** symmetry-breaking term is weak, it drives the transition from the 5D Floquet topological semimetal hosting Yang monopoles to one hosting linked Weyl surfaces. Furthermore, the stronger **TP** symmetry-breaking term can disrupt the Floquet topological phase, resulting in a transition to a trivial metal phase.

Experimentally, 5D Weyl semimetals have been realized in artificial systems such as photonic metamaterials [63], microwaves [57], and electric circuits [58, 64]. Moreover, recent experiments have shown that artificial metamaterials, such as photonic crystals [67, 130, 131, 133, 134] and electric cir-

cuits [136], are ideal platforms for realizing Floquet topological matters. Therefore, it is expected that the 5D Floquet topological semimetals can be realized based on the artificial metamaterials.

ACKNOWLEDGMENTS

B.Z. was supported by the NSFC (Grant No. 12074107), the program of outstanding young and middle-aged scientific and technological innovation team of colleges and universities in Hubei Province (Grant No. T2020001) and the innovation group project of the Natural Science Foundation of Hubei Province of China (Grant No. 2022CFA012). R.C. acknowledges the support of NSFC (under Grant No. 12304195) and the Chutian Scholars Program in Hubei Province. Z.-R.L. was supported by the National Funded Postdoctoral Researcher Program (under Grant No. GZC20230751) and the Postdoctoral Innovation Research Program in Hubei Province (under Grant No. 351342).

-
- [1] A. A. Burkov, “Topological semimetals”, *Nat. Mater.* **15**, 1145 (2016).
 - [2] B. Yan and C. Felser, “Topological materials: Weyl semimetals”, *Annu. Rev. Condens. Matter Phys.* **8**, 337 (2017).
 - [3] N. P. Armitage, E. J. Mele, and A. Vishwanath, “Weyl and Dirac semimetals in three-dimensional solids”, *Rev. Mod. Phys.* **90**, 015001 (2018).
 - [4] B. Q. Lv, T. Qian, and H. Ding, “Experimental perspective on three-dimensional topological semimetals”, *Rev. Mod. Phys.* **93**, 025002 (2021).
 - [5] H. Nielsen and M. Ninomiya, “The Adler-Bell-Jackiw anomaly and Weyl fermions in a crystal”, *Phys. Lett. B* **130**, 389 (1983).
 - [6] M. V. Berry, “Quantal phase factors accompanying adiabatic changes”, *Proc. R. Soc. A* **392**, 45 (1984).
 - [7] F. D. M. Haldane, “Berry Curvature on the Fermi Surface: Anomalous Hall Effect as a Topological Fermi-Liquid Property”, *Phys. Rev. Lett.* **93**, 206602 (2004).
 - [8] S. Murakami, “Phase transition between the quantum spin Hall and insulator phases in 3D: emergence of a topological gapless phase”, *New J. Phys.* **9**, 356 (2007).
 - [9] X. Wan, A. M. Turner, A. Vishwanath, and S. Y. Savrasov, “Topological semimetal and Fermi-arc surface states in the electronic structure of pyrochlore iridates”, *Phys. Rev. B* **83**, 205101 (2011).
 - [10] S. Murakami, M. Hirayama, R. Okugawa, and T. Miyake, “Emergence of topological semimetals in gap closing in semiconductors without inversion symmetry”, *Sci. Adv.* **3**, e1602680 (2017).
 - [11] R. Chen, B. Zhou, and D.-H. Xu, “Quasicrystalline second-order topological semimetals”, *Phys. Rev. B* **108**, 195306 (2023).
 - [12] X. Ding, X. Jin, Z. Chen, X. Lv, D.-S. Ma, X. Wu, and R. Wang, “Abundant surface-semimetal phases in three-dimensional obstructed atomic insulators”, *Phys. Rev. B* **108**, 085135 (2023).
 - [13] S.-Y. Xu, C. Liu, S. K. Kushwaha, R. Sankar, J. W. Krizan, I. Belopolski, *et al.*, “Observation of Fermi arc surface states in a topological metal”, *Science* **347**, 294 (2015).
 - [14] Z. Wang, H. Weng, Q. Wu, X. Dai, and Z. Fang, “Three-dimensional Dirac semimetal and quantum transport in Cd₃As₂”, *Phys. Rev. B* **88**, 125427 (2013).
 - [15] M. Neupane, S.-Y. Xu, R. Sankar, N. Alidoust, G. Bian, C. Liu, *et al.*, “Observation of a three-dimensional topological Dirac semimetal phase in high-mobility Cd₃As₂”, *Nat. Commun.* **5**, 3786 (2014).
 - [16] S. Jeon, B. B. Zhou, A. Gynis, B. E. Feldman, I. Kimchi, A. C. Potter, Q. D. Gibson, R. J. Cava, A. Vishwanath, and A. Yazdani, “Landau quantization and quasiparticle interference in the three-dimensional Dirac semimetal Cd₃As₂”, *Nat. Mater.* **13**, 851 (2014).
 - [17] G. Xu, H. Weng, Z. Wang, X. Dai, and Z. Fang, “Chern Semimetal and the Quantized Anomalous Hall Effect in HgCr₂Se₄”, *Phys. Rev. Lett.* **107**, 186806 (2011).
 - [18] R. Yu, H. Weng, Z. Fang, X. Dai, and X. Hu, “Topological Node-Line Semimetal and Dirac Semimetal State in Antiperovskite Cu₃PdN”, *Phys. Rev. Lett.* **115**, 036807 (2015).
 - [19] Y. Murotani, N. Kanda, T. Fujimoto, T. Matsuda, M. Goyal, J. Yoshinobu, Y. Kobayashi, T. Oka, S. Stemmer, and R. Matsunaga, “Disentangling the Competing Mechanisms of Light-Induced Anomalous Hall Conductivity in Three-Dimensional Dirac Semimetal”, *Phys. Rev. Lett.* **131**, 096901 (2023).
 - [20] T.-Y. Zhao, A.-Q. Wang, X.-G. Ye, X.-Y. Liu, X. Liao, and Z.-M. Liao, “Gate-Tunable Berry Curvature Dipole Polarizability in Dirac Semimetal Cd₃As₂”, *Phys. Rev. Lett.* **131**, 186302 (2023).
 - [21] Z. Wang, Y. Sun, X.-Q. Chen, C. Franchini, G. Xu, H. Weng, X. Dai, and Z. Fang, “Dirac semimetal and topological phase transitions in A₃bi ($a = \text{Na}, \text{k}, \text{rb}$)”, *Phys. Rev. B* **85**, 195320 (2012).

- [22] S. M. Young, S. Zaheer, J. C. Y. Teo, C. L. Kane, E. J. Mele, and A. M. Rappe, “Dirac Semimetal in Three Dimensions”, *Phys. Rev. Lett.* **108**, 140405 (2012).
- [23] S. Borisenko, Q. Gibson, D. Evtushinsky, V. Zabolotnyy, B. Büchner, and R. J. Cava, “Experimental Realization of a Three-Dimensional Dirac Semimetal”, *Phys. Rev. Lett.* **113**, 027603 (2014).
- [24] R. Chen, T. Liu, C. M. Wang, H.-Z. Lu, and X. C. Xie, “Field-Tunable One-Sided Higher-Order Topological Hinge States in Dirac Semimetals”, *Phys. Rev. Lett.* **127**, 066801 (2021).
- [25] Z. Ning, X. Ding, D.-H. Xu, and R. Wang, “Robustness of half-integer quantized Hall conductivity against disorder in an anisotropic Dirac semimetal with parity anomaly”, *Phys. Rev. B* **108**, L041104 (2023).
- [26] H. Weyl, “Elektron und Gravitation. I”, *Z. Phys.* **56**, 330 (1929).
- [27] A. A. Zyuzin and A. A. Burkov, “Topological response in Weyl semimetals and the chiral anomaly”, *Phys. Rev. B* **86**, 115133 (2012).
- [28] C.-X. Liu, P. Ye, and X.-L. Qi, “Chiral gauge field and axial anomaly in a Weyl semimetal”, *Phys. Rev. B* **87**, 235306 (2013).
- [29] D. T. Son and B. Z. Spivak, “Chiral anomaly and classical negative magnetoresistance of Weyl metals”, *Phys. Rev. B* **88**, 104412 (2013).
- [30] J. Liu and D. Vanderbilt, “Weyl semimetals from noncentrosymmetric topological insulators”, *Phys. Rev. B* **90**, 155316 (2014).
- [31] S.-Y. Xu, I. Belopolski, N. Alidoust, M. Neupane, G. Bian, C. Zhang, *et al.*, “Discovery of a Weyl fermion semimetal and topological Fermi arcs”, *Science* **349**, 613 (2015).
- [32] H. Weng, C. Fang, Z. Fang, B. A. Bernevig, and X. Dai, “Weyl Semimetal Phase in Noncentrosymmetric Transition-Metal Monophosphides”, *Phys. Rev. X* **5**, 011029 (2015).
- [33] S.-M. Huang, S.-Y. Xu, I. Belopolski, C.-C. Lee, G. Chang, B. Wang, *et al.*, “A Weyl Fermion semimetal with surface Fermi arcs in the transition metal monopnictide TaAs class”, *Nat. Commun.* **6**, 7373 (2015).
- [34] B. Q. Lv, H. M. Weng, B. B. Fu, X. P. Wang, H. Miao, J. Ma, *et al.*, “Experimental Discovery of Weyl Semimetal TaAs”, *Phys. Rev. X* **5**, 031013 (2015).
- [35] L. Balents, “Weyl electrons kiss”, *Physics* **4** (2011), 10.1103/physics.4.36.
- [36] B. W. Xia, R. Wang, Z. J. Chen, Y. J. Zhao, and H. Xu, “Symmetry-Protected Ideal Type-II Weyl Phonons in CdTe”, *Phys. Rev. Lett.* **123**, 065501 (2019).
- [37] C. Zhang, X.-Y. Ding, L.-Y. Gan, Y. Cao, B.-S. Li, X. Wu, and R. Wang, “Symmetry-guaranteed ideal Weyl semimetallic phase in face-centered orthogonal C₆”, *Phys. Rev. B* **101**, 235119 (2020).
- [38] Y. Yang, F. Yu, X. Wen, Z. Gui, Y. Zhang, F. Zhan, R. Wang, J. Ying, and X. Chen, “Pressure-induced transition from a Mott insulator to a ferromagnetic Weyl metal in La₂O₃Fe₂Se₂”, *Nat. Commun.* **14**, 2260 (2023).
- [39] N. Zhang, X. Ding, F. Zhan, H. Li, H. Li, K. Tang, *et al.*, “Temperature-dependent and magnetism-controlled Fermi surface changes in magnetic Weyl semimetals”, *Phys. Rev. Res.* **5**, L022013 (2023).
- [40] S. Fan, B. Fu, D.-S. Ma, and R. Wang, “Complete topological phase diagram and realization of minimum Weyl nodes in a sheared chiral crystal of elemental tellurium”, *Phys. Rev. B* **108**, 235211 (2023).
- [41] F. Balduini, L. Rocchino, A. Molinari, T. Paul, G. Mariani, V. Hasse, C. Felser, C. Zota, H. Schmid, and B. Gotsmann, “Probing the Shape of the Weyl Fermi Surface of NbP Using Transverse Electron Focusing”, *Phys. Rev. Lett.* **133**, 096601 (2024).
- [42] Q. Lu, P. V. S. Reddy, H. Jeon, A. R. Mazza, M. Brahlek, W. Wu, *et al.*, “Realization of a two-dimensional Weyl semimetal and topological Fermi strings”, *Nat. Commun.* **15**, 6001 (2024).
- [43] A. A. Burkov, M. D. Hook, and L. Balents, “Topological nodal semimetals”, *Phys. Rev. B* **84**, 235126 (2011).
- [44] H. Weng, Y. Liang, Q. Xu, R. Yu, Z. Fang, X. Dai, and Y. Kawazoe, “Topological node-line semimetal in three-dimensional graphene networks”, *Phys. Rev. B* **92**, 045108 (2015).
- [45] Z. Zhou, X. Yang, H. Wang, G. Han, X. Lu, G. Wang, R. Wang, and X. Zhou, “Giant phonon anomaly in topological nodal-line semimetals”, *Funda. Res.* (2022), <https://doi.org/10.1016/j.fmre.2022.12.012>.
- [46] H.-J. Lin, T. Liu, and H.-Z. Lu, “Quantum oscillations in acoustic phonons of nodal-line semimetals”, *Phys. Rev. B* **109**, 195421 (2024).
- [47] Y. Yang, R. Wang, M.-Z. Shi, Z. Wang, Z. Xiang, and X.-H. Chen, “Symmetry-protected Dirac nodal lines and large spin Hall effect in a V₆Sb₄ kagome bilayer”, *Phys. Rev. B* **105**, 155102 (2022).
- [48] H. Nielsen and M. Ninomiya, “Absence of neutrinos on a lattice: (I). Proof by homotopy theory”, *Nucl. Phys. B* **185**, 20 (1981).
- [49] H. Nielsen and M. Ninomiya, “Absence of neutrinos on a lattice: (II). Intuitive topological proof”, *Nucl. Phys. B* **193**, 173 (1981).
- [50] L. Lu, Z. Wang, D. Ye, L. Ran, L. Fu, J. D. Joannopoulos, and M. Soljačić, “Experimental observation of Weyl points”, *Science* **349**, 622 (2015).
- [51] B. Yang, Q. Guo, B. Tremain, R. Liu, L. E. Barr, Q. Yan, *et al.*, “Ideal Weyl points and helicoid surface states in artificial photonic crystal structures”, *Science* **359**, 1013 (2018).
- [52] S.-Y. Xu, N. Alidoust, I. Belopolski, Z. Yuan, G. Bian, T.-R. Chang, *et al.*, “Discovery of a Weyl fermion state with Fermi arcs in niobium arsenide”, *Nature Physics* **11**, 748 (2015).
- [53] B. Lian and S.-C. Zhang, “Five-dimensional generalization of the topological Weyl semimetal”, *Phys. Rev. B* **94**, 041105 (2016).
- [54] C. N. Yang, “Generalization of Dirac’s monopole to SU2 gauge fields”, *J. Math. Phys.* **19**, 320 (1978).
- [55] S. Sugawa, F. Salces-Carcoba, A. R. Perry, Y. Yue, and I. B. Spielman, “Second Chern number of a quantum-simulated non-Abelian Yang monopole”, *Science* **360**, 1429 (2018).
- [56] K. Hasebe, “SO(5) Landau models and nested Nambu matrix geometry”, *Nucl. Phys. B* **956**, 115012 (2020).
- [57] S. Ma, H. Jia, Y. Bi, S. Ning, F. Guan, H. Liu, C. Wang, and S. Zhang, “Gauge Field Induced Chiral Zero Mode in Five-Dimensional Yang Monopole Metamaterials”, *Phys. Rev. Lett.* **130**, 243801 (2023).
- [58] X. Zheng, T. Chen, W. Zhang, H. Sun, and X. Zhang, “Exploring topological phase transition and Weyl physics in five dimensions with electric circuits”, *Phys. Rev. Res.* **4**, 033203 (2022).
- [59] B. Lian and S.-C. Zhang, “Weyl semimetal and topological phase transition in five dimensions”, *Phys. Rev. B* **95**, 235106 (2017).
- [60] K. Hashimoto, X. Wu, and T. Kimura, “Edge states at an intersection of edges of a topological material”, *Phys. Rev. B* **95**, 165443 (2017).

- [61] J.-Y. Chen, B. Lian, and S.-C. Zhang, “Doubling theorem and boundary states of five-dimensional Weyl semimetal”, *Phys. Rev. B* **100**, 075112 (2019).
- [62] K. Hashimoto and Y. Matsuo, “Universal higher-order topology from a five-dimensional Weyl semimetal: Edge topology, edge Hamiltonian, and a nested Wilson loop”, *Phys. Rev. B* **101**, 245138 (2020).
- [63] S. Ma, Y. Bi, Q. Guo, B. Yang, O. You, J. Feng, H.-B. Sun, and S. Zhang, “Linked Weyl surfaces and Weyl arcs in photonic metamaterials”, *Science* **373**, 572 (2021).
- [64] X. Zheng, T. Chen, and X. Zhang, “Topological states in a five-dimensional non-Hermitian system”, *Phys. Rev. B* **109**, 085307 (2024).
- [65] V. Mathai and G. C. Thiang, “Differential Topology of Semimetals”, *Commun. Math. Phys.* **355**, 561 (2017).
- [66] M. Ezawa, “Electric circuit simulations of n th-Chern-number insulators in $2n$ -dimensional space and their non-Hermitian generalizations for arbitrary n ”, *Phys. Rev. B* **100**, 075423 (2019).
- [67] M. C. Rechtsman, J. M. Zeuner, Y. Plotnik, Y. Lumer, D. Podolsky, F. Dreisow, S. Nolte, M. Segev, and A. Szameit, “Photonic Floquet topological insulators”, *Nature* **496**, 196 (2013).
- [68] N. H. Lindner, G. Refael, and V. Galitski, “Floquet topological insulator in semiconductor quantum wells”, *Nat. Phys.* **7**, 490 (2011).
- [69] K. Wintersperger, C. Braun, F. N. Ünal, A. Eckardt, M. D. Liberto, N. Goldman, I. Bloch, and M. Aidelsburger, “Realization of an anomalous Floquet topological system with ultracold atoms”, *Nat. Phys.* **16**, 1058 (2020).
- [70] J. W. McIver, B. Schulte, F.-U. Stein, T. Matsuyama, G. Jotzu, G. Meier, and A. Cavalleri, “Light-induced anomalous Hall effect in graphene”, *Nat. Phys.* **16**, 38 (2019).
- [71] Z. Gu, H. A. Fertig, D. P. Arovas, and A. Auerbach, “Floquet Spectrum and Transport through an Irradiated Graphene Ribbon”, *Phys. Rev. Lett.* **107**, 216601 (2011).
- [72] D. Y. H. Ho and J. Gong, “Quantized Adiabatic Transport In Momentum Space”, *Phys. Rev. Lett.* **109**, 010601 (2012).
- [73] A. Gómez-León and G. Platero, “Floquet-Bloch Theory and Topology in Periodically Driven Lattices”, *Phys. Rev. Lett.* **110**, 200403 (2013).
- [74] A. Kundu and B. Seradjeh, “Transport Signatures of Floquet Majorana Fermions in Driven Topological Superconductors”, *Phys. Rev. Lett.* **111**, 136402 (2013).
- [75] M. Lababidi, I. I. Satija, and E. Zhao, “Counter-propagating Edge Modes and Topological Phases of a Kicked Quantum Hall System”, *Phys. Rev. Lett.* **112**, 026805 (2014).
- [76] L. E. F. Foa Torres, P. M. Perez-Piskunow, C. A. Balseiro, and G. Usaj, “Multiterminal Conductance of a Floquet Topological Insulator”, *Phys. Rev. Lett.* **113**, 266801 (2014).
- [77] C. H. Lee, W. W. Ho, B. Yang, J. Gong, and Z. Papić, “Floquet mechanism for non-abelian fractional quantum hall states”, *Phys. Rev. Lett.* **121**, 237401 (2018).
- [78] M. S. Rudner, N. H. Lindner, E. Berg, and M. Levin, “Anomalous Edge States and the Bulk-Edge Correspondence for Periodically Driven Two-Dimensional Systems”, *Phys. Rev. X* **3**, 031005 (2013).
- [79] H. Hübener, M. A. Sentef, U. De Giovannini, A. F. Kemper, and A. Rubio, “Creating stable Floquet-Weyl semimetals by laser-driving of 3D Dirac materials”, *Nat. Commun.* **8**, 13940 (2017).
- [80] M. S. Rudner and N. H. Lindner, “Band structure engineering and non-equilibrium dynamics in Floquet topological insulators”, *Nat. Rev. Phys.* **2**, 229 (2020).
- [81] A. Stegmaier, H. Brand, S. Imhof, A. Fritzsch, T. Helbig, T. Hofmann, *et al.*, “Realizing efficient topological temporal pumping in electrical circuits”, *Phys. Rev. Res.* **6**, 023010 (2024).
- [82] T. Oka and H. Aoki, “Photovoltaic Hall effect in graphene”, *Phys. Rev. B* **79**, 081406 (2009).
- [83] T. Kitagawa, E. Berg, M. Rudner, and E. Demler, “Topological characterization of periodically driven quantum systems”, *Phys. Rev. B* **82**, 235114 (2010).
- [84] J. Wang and J. Gong, “Proposal of a cold-atom realization of quantum maps with Hofstadter’s butterfly spectrum”, *Phys. Rev. A* **77**, 031405 (2008).
- [85] F. Zhan, J. Zeng, Z. Chen, X. Jin, J. Fan, T. Chen, and R. Wang, “Floquet Engineering of Nonequilibrium Valley-Polarized Quantum Anomalous Hall Effect with Tunable Chern Number”, *Nano Lett.* **23**, 2166 (2023).
- [86] M. Jangjan and M. V. Hosseini, “Floquet engineering of topological metal states and hybridization of edge states with bulk states in dimerized two-leg ladders”, *Sci. Rep.* **10**, 14256 (2020).
- [87] H. Wu and J.-H. An, “Floquet topological phases of non-Hermitian systems”, *Phys. Rev. B* **102**, 041119 (2020).
- [88] M. Jangjan, L. E. F. Foa Torres, and M. V. Hosseini, “Floquet topological phase transitions in a periodically quenched dimer”, *Phys. Rev. B* **106**, 224306 (2022).
- [89] F. Qin, C. H. Lee, and R. Chen, “Light-induced phase crossovers in a quantum spin Hall system”, *Phys. Rev. B* **106**, 235405 (2022).
- [90] H. Wu and J.-H. An, “Hybrid-order topological odd-parity superconductors via Floquet engineering”, *Phys. Rev. B* **107**, 235132 (2023).
- [91] F. Qin, C. H. Lee, and R. Chen, “Light-induced half-quantized Hall effect and axion insulator”, *Phys. Rev. B* **108**, 075435 (2023).
- [92] H. Wu, “Composite topological phases via Floquet engineering”, *Phys. Rev. B* **108**, 195125 (2023).
- [93] F. Qin, R. Chen, and H.-Z. Lu, “Phase transitions in intrinsic magnetic topological insulator with high-frequency pumping”, *J. Phys.: Condens. Matter* **34**, 225001 (2022).
- [94] J. Cayssol, B. Dóra, F. Simon, and R. Moessner, “Floquet topological insulators”, *Phys. Status Solidi RRL* **7**, 101 (2013).
- [95] H. Wu, Y.-C. Dong, and H. Liu, “Floquet topological phases with time-reversal and space-inversion symmetries and dynamical detection of topological charges”, *Phys. Rev. B* **110**, 235140 (2024).
- [96] X. Wan, Z. Ning, D.-H. Xu, R. Wang, and B. Zheng, “Photoinduced high-Chern-number quantum anomalous Hall effect from higher-order topological insulators”, *Phys. Rev. B* **109**, 085148 (2024).
- [97] F. Qin, R. Chen, and C. H. Lee, “Light-enhanced nonlinear Hall effect”, *Commun. Phys.* **7**, 368 (2024).
- [98] J.-H. Zhang, F. Mei, Y. Li, C. H. Lee, J. Ma, L. Xiao, and S. Jia, “Observation of higher-order time-dislocation topological modes”, (2024), arXiv:2406.04763 [cond-mat.mes-hall].
- [99] A. Stegmaier, A. Fritzsch, R. Sorbello, M. Greiter, H. Brand, C. Barko, *et al.*, “Topological Edge State Nucleation in Frequency Space and its Realization with Floquet Electrical Circuits”, (2024), arXiv:2407.10191 [cond-mat.mes-hall].
- [100] F. Zhan, R. Chen, Z. Ning, D.-S. Ma, Z. Wang, D.-H. Xu, and R. Wang, “Perspective: Floquet engineering topological states from effective models towards realistic materials”, *Quantum Front.* **3**, 21 (2024).
- [101] R. Wang, B. Wang, R. Shen, L. Sheng, and D. Y. Xing, “Floquet Weyl semimetal induced by off-resonant light”, *Europhys.*

- Lett. **105**, 17004 (2014).
- [102] Z. Yan and Z. Wang, “Tunable Weyl Points in Periodically Driven Nodal Line Semimetals”, *Phys. Rev. Lett.* **117**, 087402 (2016).
- [103] H. Liu, J.-T. Sun, C. Cheng, F. Liu, and S. Meng, “Photoinduced Nonequilibrium Topological States in Strained Black Phosphorus”, *Phys. Rev. Lett.* **120**, 237403 (2018).
- [104] L. Li, C. H. Lee, and J. Gong, “Realistic Floquet Semimetal with Exotic Topological Linkages between Arbitrarily Many Nodal Loops”, *Phys. Rev. Lett.* **121**, 036401 (2018).
- [105] X.-Q. Sun, M. Xiao, T. c. v. Bzdušek, S.-C. Zhang, and S. Fan, “Three-Dimensional Chiral Lattice Fermion in Floquet Systems”, *Phys. Rev. Lett.* **121**, 196401 (2018).
- [106] S. Higashikawa, M. Nakagawa, and M. Ueda, “Floquet Chiral Magnetic Effect”, *Phys. Rev. Lett.* **123**, 066403 (2019).
- [107] Y. Zhu, T. Qin, X. Yang, G. Xianlong, and Z. Liang, “Floquet and anomalous Floquet Weyl semimetals”, *Phys. Rev. Res.* **2**, 033045 (2020).
- [108] W. Zhu, M. Umer, and J. Gong, “Floquet higher-order Weyl and nexus semimetals”, *Phys. Rev. Res.* **3**, L032026 (2021).
- [109] H. Wang, L. Zhou, and Y. D. Chong, “Floquet Weyl phases in a three-dimensional network model”, *Phys. Rev. B* **93**, 144114 (2016).
- [110] L. Zhou, C. Chen, and J. Gong, “Floquet semimetal with Floquet-band holonomy”, *Phys. Rev. B* **94**, 075443 (2016).
- [111] X.-X. Zhang, T. T. Ong, and N. Nagaosa, “Theory of photoinduced Floquet Weyl semimetal phases”, *Phys. Rev. B* **94**, 235137 (2016).
- [112] C.-K. Chan, Y.-T. Oh, J. H. Han, and P. A. Lee, “Type-II Weyl cone transitions in driven semimetals”, *Phys. Rev. B* **94**, 121106 (2016).
- [113] R. W. Bomantara and J. Gong, “Generating controllable type-II Weyl points via periodic driving”, *Phys. Rev. B* **94**, 235447 (2016).
- [114] Z. Yan and Z. Wang, “Floquet multi-Weyl points in crossing-nodal-line semimetals”, *Phys. Rev. B* **96**, 041206 (2017).
- [115] M. Ezawa, “Photoinduced topological phase transition from a crossing-line nodal semimetal to a multiple-Weyl semimetal”, *Phys. Rev. B* **96**, 041205 (2017).
- [116] L. Bucciantini, S. Roy, S. Kitamura, and T. Oka, “Emergent Weyl nodes and Fermi arcs in a Floquet Weyl semimetal”, *Phys. Rev. B* **96**, 041126 (2017).
- [117] R. Chen, B. Zhou, and D.-H. Xu, “Floquet Weyl semimetals in light-irradiated type-II and hybrid line-node semimetals”, *Phys. Rev. B* **97**, 155152 (2018).
- [118] T. Deng, B. Zheng, F. Zhan, J. Fan, X. Wu, and R. Wang, “Photoinduced Floquet mixed-Weyl semimetallic phase in a carbon allotrope”, *Phys. Rev. B* **102**, 201105 (2020).
- [119] M. Umer, R. W. Bomantara, and J. Gong, “Dynamical characterization of Weyl nodes in Floquet Weyl semimetal phases”, *Phys. Rev. B* **103**, 094309 (2021).
- [120] B.-Q. Wang, H. Wu, and J.-H. An, “Engineering exotic second-order topological semimetals by periodic driving”, *Phys. Rev. B* **104**, 205117 (2021).
- [121] X.-L. Du, R. Chen, R. Wang, and D.-H. Xu, “Weyl nodes with higher-order topology in an optically driven nodal-line semimetal”, *Phys. Rev. B* **105**, L081102 (2022).
- [122] H. Wu and J.-H. An, “Non-Hermitian Weyl semimetal and its Floquet engineering”, *Phys. Rev. B* **105**, L121113 (2022).
- [123] R. Ji, X. Ding, F. Zhan, X. Xiao, J. Fan, Z. Ning, and R. Wang, “Controllable Weyl nodes and Fermi arcs in a light-irradiated carbon allotrope”, *Phys. Rev. B* **108**, 205139 (2023).
- [124] Z.-M. Wang, R. Wang, J.-H. Sun, T.-Y. Chen, and D.-H. Xu, “Floquet Weyl semimetal phases in light-irradiated higher-order topological Dirac semimetals”, *Phys. Rev. B* **107**, L121407 (2023).
- [125] S. Fan, S. Huang, Z. Chen, F. Zhan, X.-Y. Ding, D.-S. Ma, and R. Wang, “Circularly polarized light irradiated ferromagnetic MnBi₂Te₄: A possible ideal Weyl semimetal”, *Phys. Rev. B* **110**, 125204 (2024).
- [126] Y. H. Wang, H. Steinberg, P. Jarillo-Herrero, and N. Gedik, “Observation of Floquet-Bloch States on the Surface of a Topological Insulator”, *Science* **342**, 453 (2013).
- [127] G. Jotzu, M. Messer, R. Desbuquois, M. Lebrat, T. Uehlinger, D. Greif, and T. Esslinger, “Experimental realization of the topological Haldane model with ultracold fermions”, *Nature* **515**, 237 (2014).
- [128] R. Fleury, A. B. Khanikaev, and A. Alù, “Floquet topological insulators for sound”, *Nat. Commun.* **7**, 11744 (2016).
- [129] Y.-G. Peng, C.-Z. Qin, D.-G. Zhao, Y.-X. Shen, X.-Y. Xu, M. Bao, H. Jia, and X.-F. Zhu, “Experimental demonstration of anomalous Floquet topological insulator for sound”, *Nat. Commun.* **7**, 13368 (2016).
- [130] L. J. Maczewsky, J. M. Zeuner, S. Nolte, and A. Szameit, “Observation of photonic anomalous Floquet topological insulators”, *Nat. Commun.* **8**, 13756 (2017).
- [131] S. Mukherjee, A. Spracklen, M. Valiente, E. Andersson, P. Öhberg, N. Goldman, and R. R. Thomson, “Experimental observation of anomalous topological edge modes in a slowly driven photonic lattice”, *Nat. Commun.* **8**, 13918 (2017).
- [132] L. Asteria, D. T. Tran, T. Ozawa, M. Tarnowski, B. S. Rem, N. Fläschner, K. Sengstock, N. Goldman, and C. Weitenberg, “Measuring quantized circular dichroism in ultracold topological matter”, *Nat. Phys.* **15**, 449 (2019).
- [133] T. Ozawa, H. M. Price, A. Amo, N. Goldman, M. Hafezi, L. Lu, *et al.*, “Topological photonics”, *Rev. Mod. Phys.* **91**, 015006 (2019).
- [134] L. J. Maczewsky, B. Höckendorf, M. Kremer, T. Biesenthal, M. Heinrich, A. Alvermann, H. Fehske, and A. Szameit, “Fermionic time-reversal symmetry in a photonic topological insulator”, *Nat. Mater.* **19**, 855 (2020).
- [135] B. Chen, S. Li, X. Hou, F. Ge, F. Zhou, P. Qian, F. Mei, S. Jia, N. Xu, and H. Shen, “Digital quantum simulation of Floquet topological phases with a solid-state quantum simulator”, *Photon. Res.* **9**, 81 (2021).
- [136] S. S. Dabiri and H. Cheraghchi, “Electric circuit simulation of Floquet topological insulators in Fourier space”, *J. Appl. Phys.* **134**, 084303 (2023).
- [137] O. Vafek and A. Vishwanath, “Dirac Fermions in Solids: From High-T_c Cuprates and Graphene to Topological Insulators and Weyl Semimetals”, *Annu. Rev. Condens. Matter Phys.* **5**, 83 (2014).
- [138] X.-L. Qi, T. L. Hughes, and S.-C. Zhang, “Topological field theory of time-reversal invariant insulators”, *Phys. Rev. B* **78**, 195424 (2008).
- [139] M. Mochol-Grzelak, A. Dauphin, A. Celi, and M. Lewenstein, “Efficient algorithm to compute the second Chern number in four dimensional systems”, *Quantum Sci. Technol.* **4**, 014009 (2018).
- [140] R. Chen, X.-X. Yi, and B. Zhou, “Four-dimensional topological Anderson insulator with an emergent second Chern number”, *Phys. Rev. B* **108**, 085306 (2023).
- [141] H. Weisbrich, R. Klees, G. Rastelli, and W. Belzig, “Second Chern Number and Non-Abelian Berry Phase in Topological Superconducting Systems”, *PRX Quantum* **2**, 010310 (2021).
- [142] A. Chen, Y. Guan, P. M. Lenggenhager, J. Maciejko, I. Boettcher, and T. c. v. Bzdušek, “Symmetry and topology of hyperbolic Haldane models”, *Phys. Rev. B* **108**, 085114 (2023).

- [143] Z.-R. Liu, R. Chen, and B. Zhou, “Four-dimensional Floquet topological insulator with an emergent second Chern number”, [Phys. Rev. B **109**, 125303 \(2024\)](#).
- [144] Z.-R. Liu, R. Chen, and B. Zhou, “Tuning Second Chern Number in a Four-Dimensional Topological Insulator by High-Frequency Time-Periodic Driving”, [Chinese Physics Letters **41**, 047102 \(2024\)](#).
- [145] A. Bouhon, Y.-Q. Zhu, R.-J. Slager, and G. Palumbo, “Second Euler number in four-dimensional matter”, [Phys. Rev. B **110**, 195144 \(2024\)](#).
- [146] J. H. Shirley, “Solution of the Schrödinger Equation with a Hamiltonian Periodic in Time”, [Phys. Rev. **138**, B979 \(1965\)](#).
- [147] B. Zhu, Z. Tan, Y. Ke, and H. Zhong, “Dynamic winding number for Floquet topological insulators with arbitrarily driving frequencies”, [Phys. Rev. B **109**, 224315 \(2024\)](#).